DEBLURRING OF PROBABILISTIC ODFS IN QUANTITATIVE DIFFUSION MRI

Antonio Tristán-Vega[1,2]*, Santiago Aja-Fernández*[1]*, and Carl-Fredrik Westin*[2]

[1]Laboratorio de Procesado de Imagen (Spain), [2]Laboratory of Mathematics in Imaging (Boston, USA)

ABSTRACT

The Funk-Radon Transform allows to approximate the central section integral of the diffusion signal to compute probabilistic Orientation Distribution Functions (ODF) of fiber populations, provided the behavior for the b-values not acquired is known. To relax the latter demand, it has been proposed to compute instead the integral inside the disk defined in the central section by the b-value acquired. The price to pay is low-pass filtering the ODF, cropping the information it provides. We propose a method to palliate this problem with negligible computational overload. Not only it improves the accuracy in the determination of the diffusion directions, but it also refines the crossing angles that can be resolved.

Index Terms— Diffusion MRI, HARDI, ODF, OPDT.

1. INTRODUCTION

[1] Diffusion Magnetic Resonance Imaging (MRI) has become an attractive technique in neuroimaging during the last two decades, due to the possibility it grants of studying the connectivity in the white matter non-invasively. In its most common form, Diffusion Tensor Imaging (DTI) allows estimating a second order tensor at each imaged voxel, which suffices in many cases to elucidate the principal directions of diffusion [1]. However, the limitations inherent to this technique (mainly, its incapability to resolve complex neural architectures such as fiber crossings) have encouraged the appearance of a number of methodologies intended to fit more complex diffusion models [2]. Among them, High Angular Resolution Diffusion Imaging (HARDI) has experienced a great development lastly. With this acquisition philosophy, a relatively large number of sensitizing gradients in non-collinear directions are acquired, extending the standard DTI protocol.

Though the literature on HARDI is long-winded (see [2]), we are interested here in those methods based on the Funk-Radon Transform (FRT). The diffusion propagator, $P(\mathbf{R})$, i.e. the probability law driving the diffusion of water molecules, is the Fourier transform of the signal acquired by the MRI scanner, $E(\mathbf{q})$, [3]. By virtue of the central section theorem, $P(\mathbf{R})$ may be marginalized to extract its Orientation Distribution Function (ODF), $\Phi(\mathbf{r})$, by integrating $E(\mathbf{q})$ in the plane perpendicular to $\mathbf{r}$ [4, 5]. This operation may be accomplished in polar coordinates: the integration in the angular coordinate corresponds to the FRT [6], while the radial coordinate often requires some assumption on the radial behavior of $E(\mathbf{q})$ [5]. A popular supposition in this sense is that $E(\mathbf{q})$ is a negative exponential in $\|\mathbf{q}\|^2$ [2]. Though this premise allows to find good estimates of the fiber populations in most of the cases, it is not completely accurate, and it can be relaxed as shown in [4, 5] using Orientation Probability Density Transform (OPDT)-like estimators. With the OPDT proposed in [4], we only require $E(\mathbf{q})$ to behave as a negative exponential in $\|\mathbf{q}\|^2$ locally, in an environment of the $\mathbf{q}$-value actually measured by the MRI scanner, while with the cOPDT in [5] we require the radial integral of $E(\mathbf{q})$ to locally behave as an exponential integral [7]. In both cases, the key is to replace the integral in the plane perpendicular to $\mathbf{R}$ with the integral inside the disk delimited in such plane by the intersection with the sphere $\|\mathbf{q}\| = \|\mathbf{q}_0\|$. Though these techniques have proven themselves more adequate than the simple mono-exponential-based ones, the integration inside a disk instead of the whole plane introduces a low-pass filtering of the orientation information $\Phi(\mathbf{r})$, smoothing its typically peaky shape and hindering its ability to accurately depict fiber crossings.

We aim at palliating this effect by using a deconvolution approach. In section 2 we introduce a generative model for the probabilistic ODF, $\Phi(\mathbf{r})$, as a continuous mixture (convolution) of degenerated tensors (individual fiber orientations represented as singularities in the space of directions $\{\mathbf{r} \in \mathbb{R}^3 \text{ s.t } \|\mathbf{r}\| = 1\}$). In section 3 we compute the impulse response of these convolution kernels to the low-pass filtering operation inherent to the OPDT. Using this result, we develop in section 4 a framework similar to that proposed in [8]: the OPDF, the acquired signal $E(\mathbf{q})$, and the response of the elemental tensor to the low-pass filter are represented in the basis of Spherical Harmonics (SH) [7], so that we can use the Funk-Hecke theorem to compute the desired deconvolution as a simple linear manipulation of the coefficients computed for the OPDF by means of the OPDT or the cOPDT. In section 5 we show some representative results about the improvement achieved with this approach over the regular OPDT-like estimators, while in section 6 we discuss some potential benefits of our method for fiber detection, fiber tracking, and other relevant problems related to diffusion MRI.

[1]Work funded by grants: R01 MH074794, R01 MH092862, P41 RR013218, from the NIH; TEC2010-17982, from the Spanish Government; FU2010-17982 from the Spanish Government/Fulbright Committee.

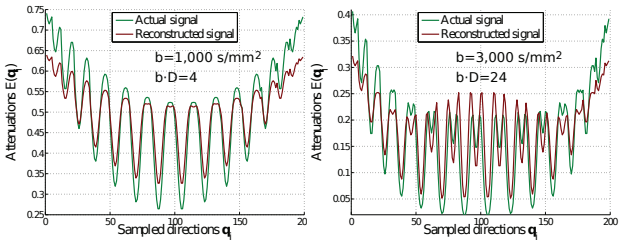


Fig. 1. Accuracy of the diffusion model proposed, for a typical scenario of two fibers crossing in an angle of 60^o. The corresponding attenuation signal $E(\mathbf{q})$ is plotted in each case against the corresponding gradient direction.

2. DIFFUSION MODEL

The signal acquired for a wave vector $\mathbf{q}$ (comprising both the pulsed gradients and the gyromagnetic ratio of the hydrogen nuclei) is related to the diffusion propagator as [3]:

$$P(\mathbf{R}) = \mathfrak{F}\left\{E(\mathbf{q})\right\}(\mathbf{R}) = \iiint_{\mathbb{R}^3} E(\mathbf{q}) \exp\left(-j2\pi \mathbf{q}^t \mathbf{R}\right) d\mathbf{q}. \quad (1)$$

In HARDI approaches, we are usually more interested in some kind of angular projection of $P(\mathbf{R})$, the so-called ODF:

$$\Phi(\mathbf{r}) = \int_0^\infty R^2 P(R\mathbf{r}) dR : \ \|\mathbf{r}\| = 1, \mathbf{R} = R\mathbf{r}, \quad (2)$$

where the term R^2 in the integral is necessary for the ODF to be an angular probability law [4]. The probabilistic ODF may be seen as a distribution of fiber orientations in the space of unit directions $\mathbf{r}$. With this consideration, our model assumes that $\Phi(\mathbf{u})$ is a prior distribution for a mixture of singular tensors: each of them has its main eigenvector (with a certain eigenvalue $\lambda > 0$) aligned with the corresponding $\mathbf{u}$, and the remaining two eigenvectors correspond to null eigenvalues:

$$P(\mathbf{R}) = \iint_{\|\mathbf{u}\|=1} \Phi(\mathbf{u}) \mathcal{P}_{\mathbf{u}}(\mathbf{R}) d\mathbf{u}, \quad (3)$$

which stands for the spherical convolution of Φ with the diffusion propagator $\mathcal{P}$ corresponding to the elemental fiber response (degenerated tensor). The $\mathcal{P}_{\mathbf{u}}$ are rotations of Gaussians aligned with the $\mathbf{z}$ axis; in Cartesian coordinates:

$$\mathcal{P}(\mathbf{R}) \equiv \mathcal{P}_{\mathbf{z}}(\mathbf{R}) = \frac{1}{\sqrt{4\pi\lambda}} \exp\left(-\frac{z^2}{4\lambda}\right) \delta(x)\delta(y). \quad (4)$$

3. LOW-PASS FILTERED ODF OF TENSORS

Eqs. (1) and (2) can be further combined to find an alternative expression of the ODF in the $\mathbf{q}$-domain [5]:

$$\Phi(\mathbf{r}) = \frac{1}{4\pi^2} - \frac{1}{8\pi^2} \iint_{\Pi} \Delta_b E(\mathbf{q}) d\mathbf{q} : \ \Pi \equiv \{\mathbf{q} : \mathbf{q} \perp \mathbf{r}\}, \quad (5)$$

where Π is the plane orthogonal to $\mathbf{r}$ that contains the origin, and Δ_b denotes the Laplace-Beltrami operator. As stated before, the most useful estimators of $\Phi(\mathbf{r})$ introduced in [4] and [5] are based on integrating an alternative domain Ω:

$$\widehat{\Phi(\mathbf{r})} = \frac{1}{4\pi^2} - \frac{1}{8\pi^2} \iint_{\Omega} \Delta_b E(\mathbf{q}) d\mathbf{q} : \\ \Omega \equiv \{\mathbf{q} : \mathbf{q} \perp \mathbf{r}, \|\mathbf{q}\| \leq q_0\}, \quad (6)$$

where q_0 is related to the b-value actually acquired by the MRI scanner [3]: $b = 4\pi^2 \tau q_0^2$. With the notation used above, and given the linearity of the spherical convolution in eq. (3), we may conclude that $\widehat{\Phi(\mathbf{r})}$ is equivalent in our model to:

$$\widehat{\Phi(\mathbf{r})} = \iint_{\|\mathbf{u}\|=1} \Phi(\mathbf{u}) \Psi_{\mathbf{u}}(\mathbf{r}) d\mathbf{u}, \quad (7)$$

where $\Psi(\mathbf{r})$ is an approximation of the ODF corresponding to the elemental tensor in eq. (4) estimated using eq. (6). To explicitly compute the rotating kernel $\Psi(\mathbf{r})$, we need the inverse Fourier transform of eq. (4), i.e. the signal theoretically acquired by the MRI scanner for a singular fiber bundle aligned with the $\mathbf{z}$ axis. In spherical coordinates, we have:

$$\mathcal{E}(\mathbf{q}) = \mathfrak{F}^{-1}\left\{\mathcal{P}(\mathbf{R})\right\}(\mathbf{q}) = \exp\left(-4\pi^2 \lambda q^2 \cos^2(\alpha)\right), \quad (8)$$

where $q = \|\mathbf{q}\|$, and α is the inclination angle of the spherical coordinates system. Since $\mathcal{E}(\mathbf{q})$ does not depend on the azimuth, the Laplace-Beltrami operator reduces to:

$$\Delta_b \mathcal{E}(\mathbf{q}) = \frac{1}{q^2 \sin(\alpha)} \frac{\partial}{\partial \alpha} \left(\sin(\alpha) \frac{\partial}{\partial \alpha} \mathcal{E}(\mathbf{q})\right) \\ = -8\pi^2 \lambda \left(1 - 8\pi^2 \lambda q^2 \cos^2\alpha \ \sin^2\alpha - 3\cos^2\alpha\right) \mathcal{E}(\mathbf{q}). \quad (9)$$

To compute the integral of eq. (9) inside Ω for each $\mathbf{r}$, we use polar coordinates. For the radial coordinate, one can use scientific calculus software to obtain:

$$\int_0^{q_0} \frac{-1}{8\pi^2} \Delta_b \mathcal{E}(\mathbf{q}) q dq = \Lambda\left(\cos(\alpha)\right); \quad (10)$$

$$\Lambda(t) = \frac{2bDt^2(1-t^2)e^{-bDt^2} - \left(1+t^2\right)\left(1-e^{-bDt^2}\right)}{8\pi^2 t^2}, \quad (11)$$

where D is the diffusivity associated to the elemental tensor ($\lambda = D\tau$). It only remains to compute the integral in the angular polar component. This reduces to computing the integral of the spherical function Λ along an equator orthogonal to each $\mathbf{r}$, i.e. computing the Funk-Radon transform of Λ [6]:

$$\Psi(\mathbf{r}) = \tfrac{1}{4\pi^2} + \mathcal{G}\left\{\Lambda(\cos\alpha)\right\}(\mathbf{r}) = \mathcal{G}\left\{\tfrac{1}{8\pi^3} + \Lambda(\cos\alpha)\right\}(\mathbf{r}). \quad (12)$$

4. DECONVOLVING THE PROBABILISTIC ODF

The ODF of the propagator in eq. (4) represents a singularity, i.e. a Dirac delta distribution, in the space of orientations-$\mathbf{r}$, corresponding to the $\mathbf{z}$ axis. In case we integrate in the whole orthogonal plane Π, eq. (7) represents a convolution with the unit element, hence the approximation is exact and $\widehat{\Phi} \equiv \Phi$. On the contrary, for the approximation in eq. (6), the low-pass filtering inherent to the integration in Ω blurs the orientation of the ODF, which is no longer a singularity. Hence, the *observed* ODF, $\widehat{\Phi}$, may be seen as the convolution

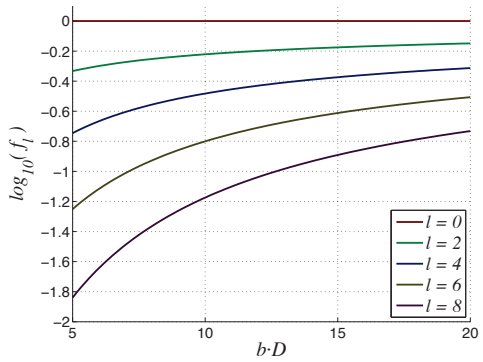


Fig. 2. Correction factors f_l, as a function of the product bD, for the first few even degrees of SH, in logarithmic scale. For $l = 0$, we have $f_0 = 1$ ($\log_{10}(f_0) = 0$) for all bD, since the probabilistic ODF has always integral 1.

of the *true* ODF we aim at computing, Φ, with the kernel Ψ. From eq. (12), it is easy to infer that $\Psi(\mathbf{r})$ depends only on the inclination angle θ in spherical coordinates, $\Psi(\mathbf{r}) = \Theta(\cos\theta)$, hence the convolution may be written in the form:

$$\widehat{\Phi(\mathbf{r})} = \iint_{\|\mathbf{u}\|=1} \Phi(\mathbf{u})\Theta(\mathbf{r}^t\mathbf{u})d\mathbf{u}. \quad (13)$$

In this situation, the Funk-Hecke theorem provides a relationship between the coefficients of $\Phi(\mathbf{r})$ in the SH basis, c_l^m, the corresponding coefficients of $\widehat{\Phi(\mathbf{r})}$, $\widehat{c_l^m}$, and the zero-order coefficients of $\Psi(\mathbf{r})$, d_l^0 (since $\Psi(\mathbf{r})$ depends only on the inclination, all other $d_l^m, m \neq 0$ are null). In precise terms:

$$\widehat{c_l^m} = \sqrt{\frac{4\pi}{2l+1}}\, d_l^0\, c_l^m \Leftrightarrow c_l^m = \sqrt{\frac{2l+1}{4\pi}}\frac{\widehat{c_l^m}}{d_l^0} = \frac{\widehat{c_l^m}}{f_l}. \quad (14)$$

Once all the functions are represented in the SH basis, the deconvolution reduces to a correction of the corresponding coefficients with the f_l. Next, we note that $\Theta(\cos\theta)$ is the FRT of $\Lambda(\cos\alpha) + 1/8\pi^3$. Since SH are eigenfunctions for the FRT with eigenvalues $\lambda_l = 2\pi(-1)^{l/2}(l-1)!!/l!!$, we may write $d_l^0 = \lambda_l\, e_l^0$, such that:

$$f_l = \sqrt{\frac{4\pi}{2l+1}}\,\lambda_l\, e_l^0 = \lambda_l \iint_{\mathbf{u}} \sqrt{\frac{4\pi}{2l+1}}\Psi(\mathbf{u})Y_l^0(\mathbf{u})d\mathbf{u}$$
$$= \frac{4\pi^2(l-1)!!}{(-1)^{l/2}l!!}\int_0^\pi \left(\frac{1}{8\pi^3} + \Lambda(\cos\alpha)\right) P_l(\cos\alpha)\sin\alpha d\alpha, \quad (15)$$

where Y_l^0 are the SH of degree-l and order-0, and P_l is the Legendre polynomial of degree-l [7]. This integral may be analytically computed with scientific software or numerically evaluated (we use the second option). **Summarizing** our approach, we use eqs. (11) and (15) to precompute (for all data sets) the correction factors f_l. These corrections are further applied to the SH coefficients of the OPDT-like estimators described in [4, 5] to remove the low-pass filtering. Note the use of SH representations is inherent to the OPDT, so the computational overload is negligible. As a final remark, note Λ in eq. (11) depends on the product bD at each voxel. We estimate it by noting that the mean value of $\mathcal{E}(\mathbf{q})$ in eq. (8) over all $\mathbf{q}$ is $\bar{\mathcal{E}} = \mathrm{erf}\sqrt{bD}/\sqrt{4\pi bD}$. Hence, if $E(\mathbf{q}_i), i = 1 \ldots N$ are the gradients acquired, we compute bD by solving:

$$\frac{\mathrm{erf}(\sqrt{bD})}{2\sqrt{\pi}\sqrt{bD}} = \frac{1}{N}\sum_{i=1}^{N} E(\mathbf{q}_i). \quad (16)$$

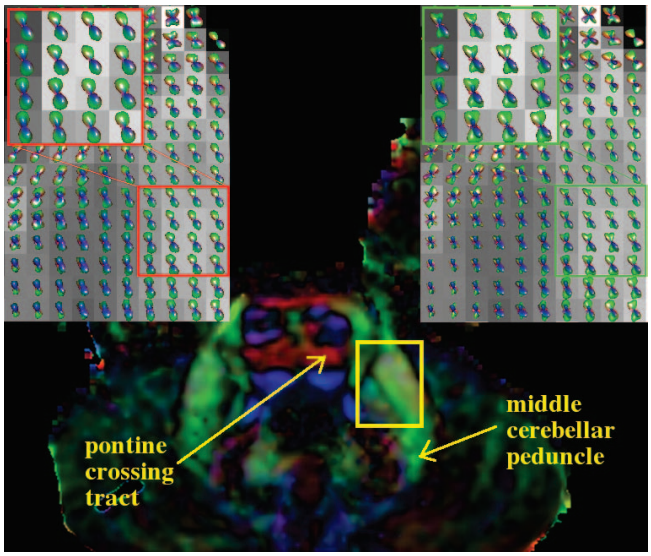


Fig. 4. Axial slice of a volunteer. The conventional cOPDT (**red**) fails to recover the crossing at the highlighted structure, while our deblurring approach (**green**) correctly resolves it.

5. RESULTS

In our first experiment we test the accuracy of the diffusion model proposed. To that end, we have simulated a noise-free signal $E(\mathbf{q})$ corresponding to a 60^o fiber crossing comprising two identical tensors with eigenvalues $[1.7, 0.3, 0.3] \times 10^{-3}$ mm^2/s, for two different b-values $b = 1,000,\ 3,000$ s/mm^2, and for 200 non-collinear directions fairly distributed in the unit sphere. The prior distribution $\Phi(\mathbf{r})$ is computed using the cOPDT in [5] and deblurred with our approach. The diffusion signal is computed convolving this ODF with the expression in eq. (8), and then compared to the true signal in Fig. 1. As it can be seen, the model described in section 2 agrees fairly well with the actual signal, justifying its use. Fig. 2 shows the correction factors f_l of the SH coefficients: the higher the degree l, the larger the amplification introduced (we divide by a smaller factor f_l), which obviously enhances the higher frequencies. To demonstrate the usefulness of this approach, we further extend our first experiment in Fig. 3 for $b = 1,000$ mm^2/s: the angle between the fibers crossing is varied within the range $[45^o, 90^o]$, and the probabilistic ODF computed with or without applying the deblurring approach presented here. Our method produces sharper ODFs that more closely resemble the ground truth analytically computed from the Gaussian mixture, allowing to resolve fiber crossings in angles as small as 45^o. Besides, when the fiber

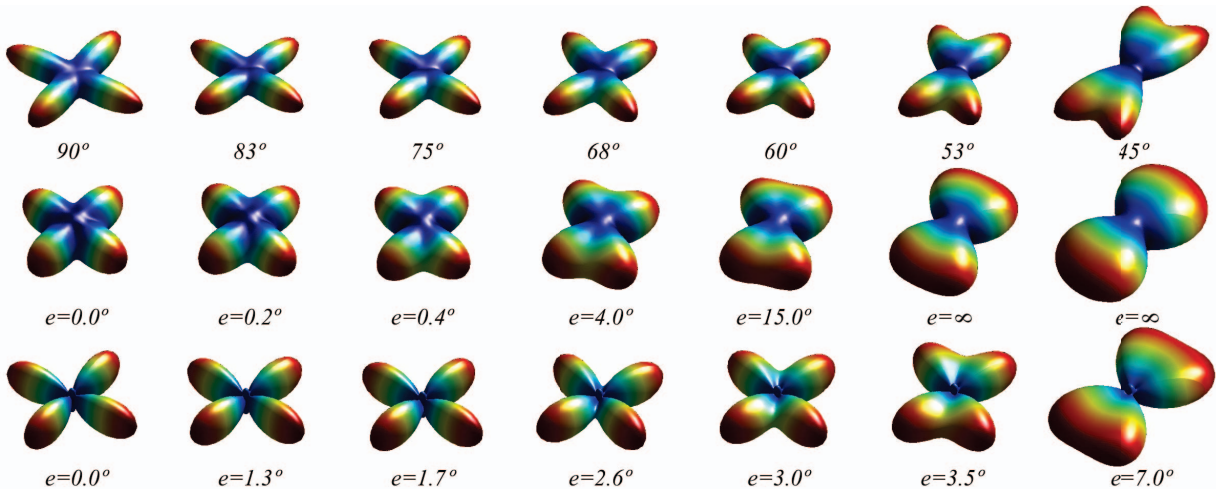


Fig. 3. Examples of probabilistic ODFs for a fiber crossing synthetically generated: (**top**) ground-truth (the number refers to the angle between the fibers); (**middle**) blurred ODF using the cOPDT approach in [5] (the angular error in the recovered fibers is indicated; ∞ means the method failed to resolve the two compartments); (**bottom**) ODF recovered after deconvolution.

directions are estimated as the local maxima of the ODFs, the error committed is far smaller after deblurring, practically for all the range. Since all the previous experiments are synthetic and do not account for side artifacts such as acquisition noise, we have conducted a final experiment with a real data set acquired in a Signa 1.5 Tesla GE Echospeed system, comprising 8 unweighted T2 baseline images and 51 diffusion weighted images with $b = 700$ s/mm^2. As it could be predicted from our previous experiment, Fig. 4 shows that the deblurring method proposed allows to resolve fiber-crossings that remain hindered when the conventional cOPDT is used. The interleaving of the fiber bundles corresponding to the middle cerebellar peduncle with those corresponding to the pontine crossing tract are typically quite difficult to resolve due to the large curvature of their trajectories. Hence, accurately deblurring the ODFs may be crucial for fiber-tracking algorithms to succeed in correctly describing these anatomies.

6. DISCUSSION AND CONCLUSIONS

OPDT-like estimators enable relaxing some common modeling assumptions in HARDI, regarding the diffusion signal for b-values not directly acquired [4, 5]. This is done at the expense of introducing a certain bias (systematic ODF blurring) whose origin is the deliberate cropping of the spectrum of the diffusion propagator. We have proposed an approach to effectively remove this artifact, so that the last theoretical limitation of OPT-like estimators compared to a mono-exponential model is overcome. In practice, the advantages of our work are also evident: fiber crossings are more accurately resolved, and we can even detect crossings that remain hindered with the regular OPDT. Furthermore, the computational overload of our proposal is negligible. Finally, our model assumes that all fiber bundles in the voxel population exhibit similar diffusivities. Future research will focus on refining this assumption, and integrating our method with sparse modeling to reduce the demands on the amount of data required [9].

7. REFERENCES

[1] P.J. Basser and C. Pierpaoli, "Microstructural and physiological features of tissues elucidated by quantitative DT-MRI," *J. Mag. Res.*, vol. 111, no. 3, pp. 209–219, 1996.

[2] H.E. Assemlal, D. Tschumperlé, L. Brun, and K. Siddiqui, "Recent advances in diffusion MRI modeling: Angular and radial reconstruction," *Med. Im. Anal.*, vol. 15, pp. 369–396, 2011.

[3] P.T. Callaghan, *Principles of Nuclear Magnetic Resonance Microscopy*, Clarendon Press, Oxford, 1991.

[4] A. Tristán-Vega, C.-F. Westin, and S. Aja-Fernández, "Estimation of fiber orientation probability density functions in HARDI," *NeuroIm.*, vol. 47, pp. 638–650, 2009.

[5] A. Tristán-Vega, C.-F. Westin, and S. Aja-Fernández, "A new methodology for the estimation of fiber populations in the white matter of the brain with the Funk-Radon transform," *NeuroIm.*, vol. 49, pp. 1301–1315, 2010.

[6] D.S. Tuch, T.G. Reese, M.R. Wiegell, and V.J. Wedeen, "Diffusion MRI of complex neural architecture," *Neuron*, vol. 40, pp. 885–895, 2003.

[7] M. Abramowitz and I. A. Stegun, Eds., *Handbook of Mathematical Functions with Formulas, Graphs, and Mathematical Tables*, Dover, New York, 1972.

[8] M. Descoteaux, R. Deriche, and A. Anwander, "Deterministic and probabilistic tractography based on complex FOD," *IEEE Trans. Med. Im.*, vol. 28, pp. 269–286, 2009.

[9] A. Tristán-Vega and C.-F. Westin, "Probabilistic ODF estimation from reduced HARDI data with sparse regularization," in *Procs. MICCAI*, 2011, pp. II.182–II.190.